Available online at www.sciencedirect.com

SCIENCE DIRECT®

Journal of Magnetism and Magnetic Materials 293 (2005) 41–47

Journal of magnetism and magnetic materials

www.elsevier.com/locate/jmmm

Characterisation of Dynabeads® by magnetization measurements and Mössbauer spectroscopy

Geir Fonnum[a,*], Christer Johansson[b], Astrid Molteberg[a], Steen Mørup[c], Elin Aksnes[a]

[a]*Dynal Biotech ASA, Post Box 114, Smestad, Ullernchausèen 52, N-309 Oslo, Norway*
[b]*IMEGO AB, Arvid Hedvalls Backe 4, SE-41133 Göteborg, Sweden*
[c]*Department of Physics, Bldg. 307, Technical University of Denmark, DK-2800 Kgs Lyngby, Denmark*

Abstract

X-ray diffraction, SEM analysis, Mössbauer spectroscopy and magnetic measurements were used to characterize three different magnetic beads (Dynabeads®). Maghemite (γ-Fe_2O_3) is the predominant crystalline phase. The nanoparticles were evenly spread in the beads, and the crystal sizes were in the range of 8 nm. The nanoparticles showed superparamagnetic behaviour. The particle's intrinsic magnetization of about 340 kA/m is typical for nanoparticles of maghemite.

Keywords: Maghemite; Nanoparticles; X-ray diffraction; SEM analysis; Mössbauer spectroscopy; Magnetic measurements; Crystallite size; Magnetic mobility; Dynabeads

---

1. Introduction

The use of magnetic beads for sample preparation of biological material and for diagnostic purposes has been a great success because of fast binding kinetics and easy handling in automated systems. The demands for magnetic beads with higher capacity and lower sedimentation rates triggered the development of smaller Dynabeads® with higher surface area. The beads that were studied are all monosized Dynabeads® of different size and iron oxide content. Dynabeads® M-280 have for a number of years been the recommended bead for in vitro diagnostic purposes and Dynabeads® M-450 has been the preferred bead-of-choice for cell separations. The new 1 μm bead Dynabeads® MyOne™ is aimed at being the preferred bead for higher capacity applications. The capacity for biotinylated Immunoglobulin on Dynabeads® MyOne™ Tosyl coated with Streptavidine is increased to 11–12 μg/mg from 3.5–4.0 μg/mg for M-280. The major challenge

---

*Corresponding author. Fax: +47 22 06 12 41.
E-mail address: geir.fonnum@dynalbiotech.com (G. Fonnum).

0304-8853/$ - see front matter © 2005 Elsevier B.V. All rights reserved.
doi:10.1016/j.jmmm.2005.01.041

with smaller beads is that a higher fraction of magnetic material is required to maintain the same mobility in a magnetic field. In this study we wanted to find out if the higher fraction of iron oxide changed the size and size distribution of the nanoparticles in the bead, and thereby the magnetic properties of the MyOne^{TM} beads compared to the other studied beads (M-280 and M-450).

Other studies of determining the sizes of single domains in other magnetic particles using different analysis techniques (magnetic measurement, Mössbauer spectroscopy, transmission electron microscopy and X-ray diffraction) have been performed earlier [1]. The result from this study showed that the determined particle size was in the same range for all of the used techniques for a specific particle system.

2. Experimental

The beads were all made by incorporation of iron oxides in porous monosized polymer beads followed by coating with a layer of polymer without charged groups [2]. The beads are characterized by the parameters given in Table 1. The mean diameter of the beads and the size distributions were determined by the method of electrical sensing zone with Beckman Coulter Multisizer 3 and the iron content by inductively coupled plasma atomic emission spectrometry (ICP-AES) after digestion.

X-ray diffraction measurements were carried out using a Siemens D5000 diffractometer in reflection geometry with a CuK$_{\alpha;}$ source and a scintillation counter.

The microstructure was investigated in a LEO Ultra 55 high-resolution field emission scanning electron microscope (FEG-SEM) in the secondary electron (SE) mode. The accelerating voltage was set to 3 kV to minimize charging effects during the analysis. Mössbauer spectra were obtained using constant acceleration Mössbauer spectrometers with sources of ^{57}Co in rhodium. Low-temperature spectra were recorded by use of a closed cycle helium refrigerator (APD Cryogenics Inc.). Spectra with applied magnetic fields were obtained by using an electromagnet with iron core. Velocities are given relative to the centroid of the spectrum of a 12.5 μm α-Fe foil, which was used for calibration.

Magnetic measurements were performed using a vibrating sample magnetometer (VSM) from LakeShore Ltd. The samples were in the form of powder and were placed in Teflon sample holders. The magnetic measurements (hysteresis loops) were carried out in the field region of ±1 T at room temperature. At 1 T the magnetization of the sample were almost saturated.

The magnetic mobility was measured by dispersing 5 mg magnetic beads coated with Streptavidin in 5.00 ml of 50.0 w% aqueous glycerol in a 10 ml polypropylene tube. The tubes were placed at exactly the same position on a Dynal MPC-6 magnet. After 0–150 s the whole dispersion was withdrawn by a pipette, leaving the beads that were drawn to the tube wall. The bead dispersion was analysed by UV/visible spectroscopy for

Table 1
Results of the characterized magnetic beads

Bead	Diameter (μm)	CV (%)	Density (g/cm^3)	Iron (mg/g)	$\chi 10^{-5}$ (m^3/kg)	M$_0$ (Am^2/kg)	Ms (kA/m)	D$_M$ (nm)	D$_X$ (nm)
M-280	2.83	1.4	1,4	118	54	10.8	336	7.8	8.1
M-450	4.40	1.2	1,6	202	102	19.6	353	7.5	8.5
MyOne^{TM}	1.05	1.9	1,7	255	81	23.5	336	7.4	7.7

CV is the standard deviation in the bead diameter given as percentage of the mean bead diameter. χ is the initial magnetic susceptibility determined from the magnetic analysis, M_0 is the mass saturation magnetization of the sample, M_s is the intrinsic spontaneous magnetization of the nanoparticles in the beads calculated as described in the text, D_M is the nanoparticle size as determined by magnetic analysis and D_X is the nanoparticle size as determined by X-ray diffraction analysis.

quantification. Each bead type needed a calibration curve.

3. Results and discussion

The X-ray diffractograms showed diffraction lines corresponding to γ-Fe_2O_3 or Fe_3O_4, which both have spinel structure and almost identical lattice constants. A detailed analysis of the line positions in the diffractogram of M-450 gave results in favour of γ-Fe_2O_3 rather than Fe_3O_4. The nanoparticle size was estimated from the Scherrer equation using the integral width, i.e. the total area under the studied diffraction peak divided by the peak maximum [3]. The results are given in Table 1. Although the iron concentration varies by more than a factor of two in the samples (see Table 1) all the samples have a similar crystal size of about 8 nm.

In Fig. 1 two SEM pictures of the M-280 magnetic bead at two magnifications can be seen. The pictures show a cross-section in the middle of the magnetic bead. The iron oxide nanoparticles in the magnetic bead are visualized in SEM pictures as bright points.

The figure shows that the iron oxide nanoparticles in the magnetic beads are distributed randomly in the pores of the M-280 beads. The same behaviour can also be seen for the M-450 beads. Some of the nanoparticles in the magnetic bead form clusters with a cluster size typically in the 20 nm range. Individual nanoparticles in the magnetic beads can be estimated from Fig. 1 to have sizes from about 6 to 12 nm.

Mössbauer spectroscopy is very sensitive to superparamagnetic relaxation in magnetic nanoparticles when the relaxation time is of the same order of magnitude as the time scale of Mössbauer spectroscopy (~a few nanoseconds). For longer relaxation times the spectra are magnetically split, i.e. they consist of sextets. For shorter relaxation times, the magnetic splitting collapses and the spectra consist of doublets or singlets. For non-interacting magnetic nanoparticles, Mössbauer spectra normally consist of a superposition of sextets and doublets or singlets due to the distribution of relaxation times related to the particle size distribution. However, interacting nanoparticles typically give rise to broadened sextets with less tendency for the presence of doublets or singlets [4,5].

Mössbauer spectra of the samples M-280 and MyOne^{TM} are shown in Fig. 2. At 20 K, the spectra of both samples are asymmetric sextets, with line 1 more intense and narrower than line 6. For both samples, the average magnetic hyperfine field is 51.4 ± 0.2 T, the average isomer shift is $0.44 \pm 0.02\,\mathrm{mm\,s^{-1}}$ and the quadrupole shift is negligible. These parameters, as well as the asymmetry, are typical for maghemite [4,6]. The asymmetry in the spectra is explained by the presence of iron in both A and B sites of the spinel lattice, which have slightly different Mössbauer

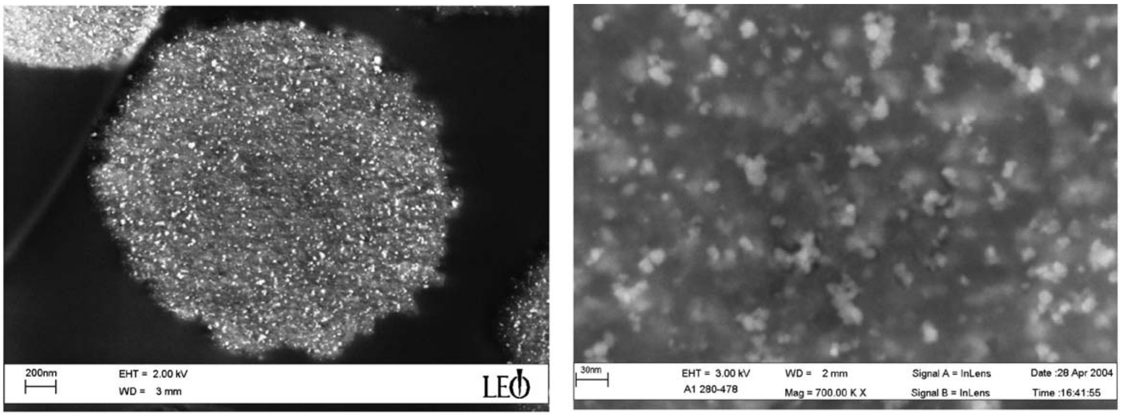

Fig. 1. SEM pictures of a M-280 bead at two different magnifications. The nanoparticles in the bead are visualized as bright points.

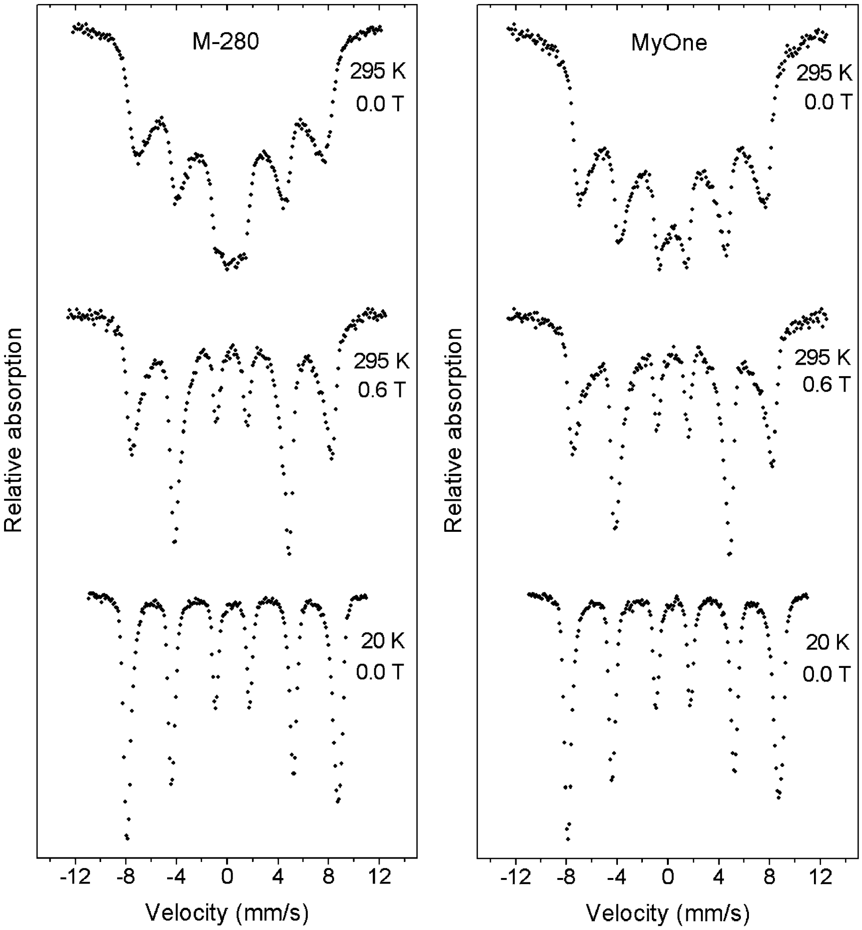

Fig. 2. Mössbauer spectrum of M-280 and MyOne^{TM} at different temperatures and magnetic fields.

parameters [6]. It was estimated that less than 1% of the iron is present in nonmagnetic phases. Mössbauer spectra, obtained at 80 K (not shown) are very similar to those obtained at 20 K.

The spectra of both samples, obtained in zero magnetic field at 295 K, show a substantial broadening, which is typical for magnetic nanoparticles in which the magnetization direction fluctuates. The spectral shape suggests that the magnetic fluctuations are influenced by inter-particle interactions [4,5]. The spectra obtained in an applied magnetic field of 0.6 T have much better resolved lines, indicating that the relaxation is suppressed in the relatively small field, as one should expect [4]. In these spectra there are no indications of other (e.g. paramagnetic) components. This shows, in accordance with the low-temperature spectra, that essentially all the iron is present in the magnetic oxide phase. Zero-field Mössbauer spectra of weakly interacting maghemite particles with average diameters of 7.5 [4] and 8.7 nm [7] have much more intense central components at room temperature than the present samples. Therefore, it can be concluded that the magnetic properties of the iron oxide nanoparticles in Dynabeads$^{®}$ are strongly influenced by inter-particle interactions. This is in accordance with the observation of clusters of particles in the SEM images. In the spectrum of M-280 there seems to be a weak central component such that lines 3 and 4 of the sextet are not resolved, but in the spectrum of MyOne^{TM}, lines 3 and 4 are well resolved, and there is no indication of a central component. This suggests that the particles in MyOne^{TM} are slightly more influenced by inter-particle interactions than the particles in M-280, but the difference is not as large as one might expect considering that the iron concentration in MyOne^{TM} is more than twice that of M-280. The Mössbauer spectra of M-450 are similar to those shown in Fig. 2, but the zero field room temperature spectra are slightly better resolved than the spectrum of MyOne^{TM}, indicating slightly stronger inter-particle interactions.

Room temperature hysteresis loops of the samples M-280 and M-450 in different field regions can be seen in Fig. 3. The samples were in the form of powder, i.e. the magnetic beads cannot rotate. This means that only the internal magnetization process (the rotation of the magnetization vector in the nanoparticles, i.e. the Néel relaxation) in the magnetic nanoparticles is measured.

From Fig. 3, it can be seen that the hysteresis loops show no remanence and no coercivity, which means that the magnetic nanoparticles in the beads are superparamagnetic as analysed with magnetic measurements with a timescale of about 10 s. Similar results were also obtained for the MyOne^{TM} magnetic beads. Magnetic beads should not show remanence since this may lead to clustering of beads during use. Remanence in nanoparticle systems is due to thermally blocked nanoparticles in the beads. The absence of remanence shows that the inter-particle interactions in the clusters of maghemite nanoparticles are insufficient to lead to blocking of the magnetization at a time scale of seconds.

For non-interacting nanoparticles, for which the magnetic anisotropy can be neglected, it is possible to estimate the particle size and size distribution by fitting magnetization data to a simple model [9]. However, in the present work, this way of determining the particle size gives only very approximate values, since magnetic interactions and magnetic anisotropy influence the magnetization [8,10]. The SEM pictures show that a large fraction of the nanoparticles in the beads form clusters, in which magnetic interactions between the nanoparticles can be significant. The results from the Mössbauer analysis also indicate magnetic interactions between the nanoparticles in the bead. However, by fitting the magnetization at higher fields, where the influence of magnetic interactions between the nanoparticles and the magnetic anisotropy of the nanoparticles is less, the sizes of the nanoparticles might be determined more accurately. The high field expression of the magnetization gives the following equation:

$$M = M_0\left(1 - \frac{kT}{M_s\langle V\rangle B}\right), \quad (1)$$

where M_0 is the saturation magnetization of the sample, k the Boltzmann constant, T the temperature, B the magnetic field and $\langle V\rangle$ is the mean volume of the nanoparticles. In Eq. (1) we have neglected other possible contributions to the

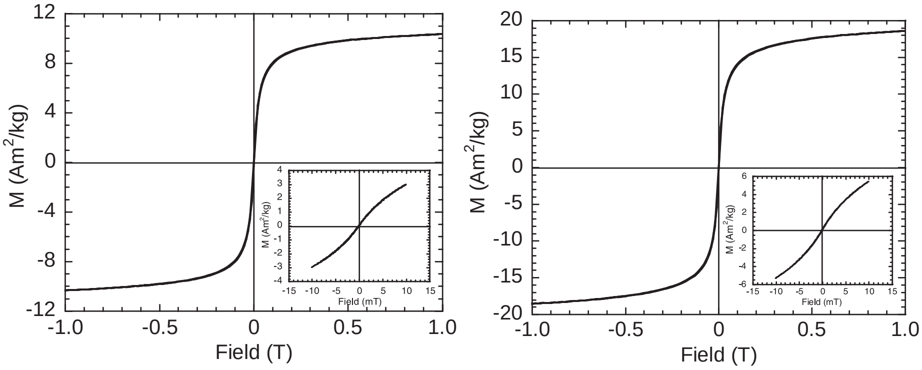

Fig. 3. Hysteresis loops (magnetization versus magnetic field) at room temperature for M-280 (left) and M-450 (right) in the field range ±1 T. Inset figures show the hysteresis loops in the field range ±10 mT.

increase in the magnetization at high fields (high-field susceptibility), which may be important at fields higher than about 2 T [8]. Fitting the magnetization data at fields up to 1 T to Eq. (1) resulted in nanoparticle sizes (as calculated from the mean volume), which are close to those obtained from X-ray diffraction (see Table 1). From the magnetic measurements it is also possible to determine the intrinsic spontaneous magnetization per volume unit, M_s, of the nanoparticles in the beads. From the high-field data of the magnetization and using Eq. (1), we calculated M_s from the values of M_0 assuming that the nanoparticles consist of maghemite. The results are given in Table 1. These values of M_s are typical for nanoparticles of maghemite [8]. The initial magnetic susceptibility was also determined from the hysteresis loops (see Table 1).

The magnetic moment of the bead and the field gradient from the separation magnet determines the magnetic force on the bead in the magnetic separation process. The acceleration, a_x, of the bead in the x-direction in a magnetic separation process, can be approximated by (assuming only magnetic field components in the x-direction)

$$a_x = \frac{\mathrm{d}^2x}{\mathrm{d}t^2} = M(B)\frac{\mathrm{d}B_x}{\mathrm{d}x} - \frac{6\pi\eta r}{m}\frac{\mathrm{d}x}{\mathrm{d}t}, \tag{2}$$

where m is the mass of the bead, $M(B)$ is the mass magnetization, r the radius of the bead and $\mathrm{d}B_x/\mathrm{d}x$ is the magnetic field gradient in the x-direction due to the permanent magnet. In Eq. (2) the frictional force on the bead is approximated by Stoke's law ($6\pi\eta r\,\mathrm{d}x/\mathrm{d}t$). The stochastic Brownian motion on the bead becomes less important at large bead sizes (larger than about 1 μm) and is not included in Eq. (2). It is seen that the total acceleration of the bead is directly related to the mass magnetization of the magnetic beads (which is dependent on the magnetic field at the beads), the field gradient from the permanent magnet and on the frictional force on the bead. In order to have a high total acceleration of the bead (which shortens the separation time) the magnetization and magnetic field gradient should be as high as possible and the size of the magnetic bead should not be to small. The magnetization curve or the hysteresis loop (see Fig. 3) gives directly the value of $M(B)$ at a specific magnetic field, B. It is only at low magnetic fields the magnetization varies linearly with the magnetic field. When a bead travels towards the permanent magnet in the separation tube the magnetic field at the bead position increases. At the surface of the separation tube the magnetic field can be as high as 0.3–0.4 T depending on the geometry and material of the permanent magnet. From Fig. 3 we can see that at these fields, the magnetization is far from varying linearly with the magnetic field. Thus, it is important to measure the whole magnetization curve, not only the initial magnetic susceptibility at low fields (where the magnetization varies linearly with the magnetic field) in order to optimise the magnetic force on the beads.

The magnetic mobilities of the three beads are shown in Fig. 4. Since the separation is very fast, glycerol was added to increase the viscosity to 6.0 mPa s [11] to slow down the process. Differences in the magnetic mobility of beads can be explained by differences in mass of the beads, frictional forces on the magnetic bead and the mass magnetization (which depends on the maghemite content). The highest mass magnetization of these three magnetic beads was obtained for the MyOne$^{\mathrm{TM}}$ bead. This means that the magnetic force on the magnetic bead in a magnetic separation process is highest for MyOne$^{\mathrm{TM}}$ among

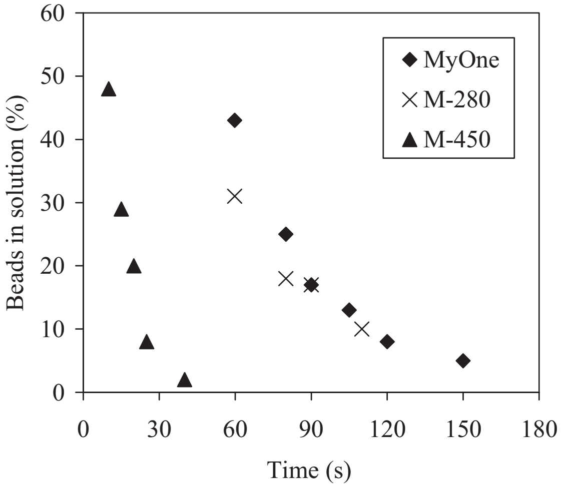

Fig. 4. Magnetic mobility data of the M-450, M-280 and the MyOne$^{\mathrm{TM}}$ magnetic bead system.

these three magnetic bead systems. However, this does not mean that the separation time is smallest for the MyOne$^{\mathrm{TM}}$ magnetic bead system. Since the frictional force, approximated by the Stoke's law, varies as the radius of the bead, r, and the mass of the beads varies as ρr^3 (where ρ is the density of the bead) the frictional force per bead mass varies as $1/\rho r^2$. Thus, the ratio of the frictional force per bead mass between the MyOne$^{\mathrm{TM}}$ bead and the M-280 and the M-450 beads is about 6 and 17, respectively (the values in Table 1 was used for the respective bead systems). This means that the deacceleration of the MyOne$^{\mathrm{TM}}$ bead (due to frictional forces) is increased by the same ratios compared to the M-280 and M-450 bead. Since the mass magnetization is almost the same for M-450 bead and the MyOne$^{\mathrm{TM}}$ bead (see Table 1), the separation time should be approximately 17 times larger for MyOne$^{\mathrm{TM}}$ than for M-450.This was found by solving the equation of bead motion taken into account the magnetic force and frictional force of an individual bead (Eq. (2)). However, from Fig. 4 it can bee seen that the separation time for MyOne$^{\mathrm{TM}}$ is only about 4 times the separation time for M-450. This value can be explained by building up of clusters of beads (that increases the total size) during the separation process. We have seen clustering of beads during the separation process by optical microscopy.

4. Conclusion

The present studies of Dynabeads® have shown that the magnetic nanoparticles consist of maghemite with a particle size of about 8 nm in the three types of beads, and there is good agreement between the particle sizes determined by magnetic analysis, SEM and X-ray diffraction. The SEM studies show that the magnetic nanoparticles are randomly distributed in the pores of the beads, but there is some tendency of clustering. The values of the intrinsic spontaneous magnetization, M_s, in Table 1 are typical for nanoparticles of maghemite [8]. Magnetization measurements showed that the nanoparticles are superparamagnetic at a time scale of seconds. Mössbauer spectroscopy studies showed that they are partially blocked at a time scale of nanoseconds, presumably because of interparticle interactions.

The separation times scales almost as $1/(M_0 \rho r)$, where M_0 is the saturation mass magnetization and r is the bead radius. The type of analyses reported in this paper is of great importance for optimising the magnetic separation process using magnetic beads.

Acknowledgements

The X-ray work have been performed by Anja Olafsen at SINTEF Materials and Chemistry, Norway, and the SEM work by Johan Angenete, MACH (Material Analysis at Chalmers), Chalmers University of Technology, Göteborg, Sweden. Diem Tran at Dynal Biotech ASA measured magnetic mobility.

References

[1] C.E. Sjøgren, C. Johansson, A. Nævestad, et al., Magn. Reson. Imaging 15 (1997) 55.
[2] J. Ugelstad, A. Rembaum, J.T. Kemshead, et al., in: S.S. Davies, L. Illum, et al. (Eds.), Microspheres and Drug Therapy, Immunological and Medical Aspects, Elsevier, Amsterdam, 1984, pp. 365–382.
[3] W.L. Smith, J. Appl. Cryst. 5 (1972) 127.
[4] S. Mørup, F. Bødker, P.V. Hendriksen, S. Linderoth, Phys. Rev. B 52 (1995) 287.
[5] C. Frandsen, S. Mørup, J. Magn. Magn. Mater. 266 (2003) 36.
[6] R.J. Pollard, Hyperfine Interact. 41 (1988) 509.
[7] S. Mørup, E. Tronc, Phys. Rev. Lett. 72 (1994) 3278.
[8] C. Johansson, M. Hanson, M.S. Pedersen, S. Mørup, J. Magn. Magn. Mater. 173 (1997) 5.
[9] R.W. Chantrell, J. Poppleweel, S.W. Charles, IEEE Trans. Magn. MAG-14 (1978) 975.
[10] M. Hanson, C. Johansson, S. Mørup, J. Phys.: Condens. Matter 5 (1993) 725.
[11] D.R. Lide (Ed.), Handbook of Chemistry and Physics, 79th ed, CRC Press, Boca Raton, FL, 1998.